

Comparative study of high temperature anti-oxidation property of sputtering deposited stoichiometric and Si-rich SiC films

Hang-Hang Wang(王行行), Wen-Qi Lu(陆文琪), Jiao Zhang(张娇), and Jun Xu(徐军)
Citation: Chin. Phys. B, 2022, 31 (**4**): 048103. DOI: 10.1088/1674-1056/ac3a61
Journal homepage: http://cpb.iphy.ac.cn; http://iopscience.iop.org/cpb

What follows is a list of articles you may be interested in

Phase-field modeling of faceted growth in solidification of alloys

Hui Xing(邢辉), Qi An(安琪), Xianglei Dong(董祥雷), and Yongsheng Han(韩永生)
Chin. Phys. B, 2022, 31 (**4**): 048104. DOI: 10.1088/1674-1056/ac3398

Comparative study of high temperature anti-oxidation property of sputtering deposited stoichiometric and Si-rich SiC films

Hang-Hang Wang(王行行), Wen-Qi Lu(陆文琪), Jiao Zhang(张娇), and Jun Xu(徐军)
Chin. Phys. B, 2022, 31 (**4**): 048103. DOI: 10.1088/1674-1056/ac3a61

Edge assisted epitaxy of $CsPbBr_3$ nanoplates on Bi_2O_2Se nanosheets for enhanced photoresponse

Haotian Jiang(蒋浩天), Xing Xu(徐兴), Chao Fan(樊超), Beibei Dai(代贝贝),Zhuodong Qi(亓卓栋), Sha Jiang(蒋莎), Mengqiu Cai(蔡孟秋), and Qinglin Zhang(张清林)
Chin. Phys. B, 2022, 31 (**4**): 048102. DOI: 10.1088/1674-1056/ac2b20

Characterization of the N-polar GaN film grown on C-plane sapphire and misoriented C-plane sapphire substrates by MOCVD

Xiaotao Hu(胡小涛), Yimeng Song(宋祎萌), Zhaole Su(苏兆乐), Haiqiang Jia(贾海强), Wenxin Wang(王文新), Yang Jiang(江洋), Yangfeng Li(李阳锋), and Hong Chen(陈弘)
Chin. Phys. B, 2022, 31 (**3**): 038103. DOI: 10.1088/1674-1056/ac3bad

A high-quality-factor ultra-narrowband perfect metamaterial absorber based on monolayer molybdenum disulfide

Liying Jiang(蒋黎英), Yingting Yi(易颖婷), Yijun Tang(唐轶峻), Zhiyou Li(李治友),Zao Yi(易早), Li Liu(刘莉), Xifang Chen(陈喜芳), Ronghua Jian(简荣华),Pinghui Wu(吴平辉), and Peiguang Yan(闫培光)
Chin. Phys. B, 2022, 31 (**3**): 038101. DOI: 10.1088/1674-1056/ac1e11

Comparative study of high temperature anti-oxidation property of sputtering deposited stoichiometric and Si-rich SiC films

Hang-Hang Wang(王行行), Wen-Qi Lu(陆文琪), Jiao Zhang(张娇), and Jun Xu(徐军)†

Key Laboratory of Materials Modification by Laser, Ion and Electron Beams, Ministry of Education, School of Physics, Dalian University of Technology, Dalian 116024, *China*

(Received 17 September 2021; revised manuscript received 31 October 2021; accepted manuscript online 17 November 2021)

Stoichiometric and silicon-rich (Si-rich) SiC films were deposited by microwave electron cyclotron resonance (MW-ECR) plasma enhanced RF magnetron sputtering method. As-deposited films were oxidized at 800 °C, 900 °C, and 1000 °C in air for 60 min. The chemical composition and structure of the films were analyzed by x-ray photoelectron spectroscopy (XPS), Raman spectroscopy and Fourier transform infrared spectroscopy (FT-IR). The surface morphology of the films before and after the high temperature oxidation was measured by atomic force microscopy. The mechanical property of the films was measured by a nano-indenter. The anti-oxidation temperature of the Si-rich SiC film is 100 °C higher than that of the stoichiometric SiC film. The oxidation layer thickness of the Si-rich SiC film is thinner than that of the stoichiometric SiC film in depth direction. The large amount of extra silicon in the Si-rich SiC film plays an important role in the improvement of its high temperature anti-oxidation property.

Keywords: SiC, anti-oxidation, silicon-rich, sputtering

PACS: 81.15.Cd, 68.60.Dv **DOI:** 10.1088/1674-1056/ac3a61

1. Introduction

Due to the excellent properties, such as low density, high melting point, good mechanical and thermal properties, excellent oxidation and chemical stability, and unique semiconductive nature, SiC and related materials have been applied in many different fields, such as aerospace, aviation, military, nuclear, chemical and semiconductor industries.[1–7] On the other hand, carbon fiber and carbon/carbon (C/C) composites have also become attractive materials with many excellent properties applicable in the aerospace and automotive manufacturing fields.[8] However, carbon fiber and C/C composites start to oxidize at 500 °C in an oxygen-containing atmosphere environment, which limits their applications in high-temperature oxidizing environments.[8,9] A solution to this problem is to coat the carbon fiber and C/C composites with an anti-oxidation layer. An ideal candidate for this anti-oxidation layer can be SiC, due to its excellent anti-oxidation property as well as good physical-chemical compatibility with carbon materials. Thus, it is necessary to investigate the high-temperature anti-oxidation property of SiC films in an oxygen-containing atmosphere environment.

Some works had been done on the oxidation of hydrogenated amorphous $Si_{1-x}C_x$ (a-$Si_{1-x}C_x$:H) films.[10–12] Authors demonstrated that the incorporation of the CH_3 radicals introduced void defects and increased the porosity of a-$Si_{1-x}C_x$:H films, which provided the necessary porous structure for oxide growth.[10,11] The a-$Si_{1-x}C_x$:H films reported by Refs. [10,11] with a large number of CH_3 radicals started to oxidize at lower temperature 200 °C and 400 °C in oxygen-containing environments, respectively. The oxidation of a-SiC:H and a-SiC in wet argon and dry oxygen atmospheres was also studied and the researchers demonstrated that the low-density a-SiC:H films with hydrogen related void defects have lower oxidation temperature than that of the high-density a-SiC films.[12] Furthermore, the high-temperature anti-oxidation property of Si–SiC coatings fabricated by impregnation-pyrolysis combined with gaseous silicon infiltration (GSI) had been reported.[13] Authors demonstrated that the structural defects in the Si–SiC coatings were filled with residual silicon after GSI process, thus resulting in the formation of dense coating, and the anti-oxidation property of SiC coating was improved.[13]

It is shown above that the hydrogen related void defects can reduce the high-temperature anti-oxidation property of SiC films. In order to improve the high-temperature anti-oxidation property and investigate the high-temperature anti-oxidation mechanism of SiC film, the unhydrogenated stoichiometric SiC and Si-rich SiC films were deposited by MW-ECR plasma enhanced RF magnetron sputtering system. The as-deposited films were oxidized at 800 °C, 900 °C and 1000 °C in air for 60 min and the anti-oxidation property of the oxidation films was characterized by FT-IR spectra and hardness-indentation depth distribution curves. Through the comparative study of the anti-oxidation property and mechanism of the stoichiometric and Si-rich SiC films, the mechanism of extra silicon in the oxidation process was briefly explained.

†Corresponding author. E-mail: xujun@dlut.edu.cn

© 2022 Chinese Physical Society and IOP Publishing Ltd

2. Experimental details

The stoichiometric and Si-rich SiC films were deposited on Si substrates by MW-ECR plasma enhanced RF magnetron sputtering system, the deposition system schematic is shown in Fig. 1 and the detailed description of the deposition system could be found in our previous publications.[14–16] In this system, the dense and highly ionized ECR plasmas are confined in the low magnetic field region between the magnetron targets and the sample table by the cusped magnetic field. The high density ECR plasmas on the SiC film surface is beneficial to the formation of Si–C bonds in SiC films.

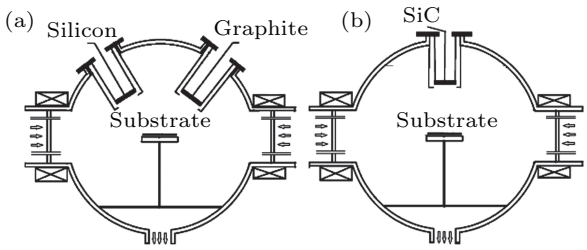


Fig. 1. The schematic diagram of the silicon and graphite co-sputtering system (a) and the ceramic SiC sputtering system (b).

The Si-rich SiC films were deposited by co-sputtering the silicon (diameter: 68 mm, purity: 99.99%) and the graphite (68 mm, 99.99%) targets. The stoichiometric SiC films were deposited by using a ceramic SiC target (68 mm, 99.9%). Before introducing the sputtering gas, the system was pumped to a pressure of 3.5×10^{-3} Pa. The flow rate of the sputtering argon gas (99.999%) was kept constant at 24 sccm and the working pressure was controlled by rotating the gate valve of molecular pump. Two microwave ECR plasma sources were both set as 500 W to get high density plasmas near the substrates and maintain discharge during sputtering process. The deposition time for all films was 120 min. For the deposition of the Si-rich SiC films, the RF power on the silicon and graphite targets was set to be 200 W and 300 W, respectively. And the working pressure was 0.22 Pa. Both distances between the silicon and graphite targets to the substrate were 150 mm. For the deposition of the stoichiometric SiC films, the RF power of the ceramic SiC target was set to be 450 W, the working pressure was 0.5 Pa and the target-substrate distance was 150 mm. The as-deposited films were oxidized at 800 °C, 900 °C and 1000 °C in air for 60 min.

The chemical composition and structure of the stoichiometric and Si-rich SiC films were analyzed by an ESCALABTM 250Xi x-ray photoelectron spectrometer. All the XPS spectra of the films were fitted with Gaussian functions and the background was removed by the Shirley subtraction method. The composition of the films can be calculated from[17]

$$C_X = \left(\frac{A_X}{S_X}\right) \Big/ \sum_{i=1}^{N} \left(\frac{A_i}{S_i}\right), \tag{1}$$

where i is the element of the film, C_X is the relative content of the X element, A is the peak area of corresponding element in the spectrum and S is the sensitivity factor of corresponding element.

The Raman spectra of the films were measured by a Renishaw inVia instrument with a 532 nm line laser as the exciting source. The infrared absorption spectra of the films were measured by a Nicolet 6700 FT-IR spectrometer in the wavenumber range of 400 cm^{-1} to 4000 cm^{-1} with a spectral resolution of 4 cm^{-1}. The mechanical property of the films was measured by an MTS Nano-indenter XP. The surface morphology of the films was measured by a CSPM 5500 atomic force microscope (AFM) with tapping mode.

3. Results and discussion

3.1. XPS characterization

The composition and Si/C ratio of the as-deposited stoichiometric and Si-rich SiC films obtained from XPS characterization are shown in Table 1. The SiC film deposited by co-sputtering is silicon rich and the Si/C ratio is 4.1, the SiC film deposited by ceramic target sputtering is stoichiometric and the Si/C ratio is 1. It is also shown that the stoichiometric SiC film has a slightly higher concentration of N and O atoms than that of the Si-rich SiC film.

Table 1. The composition and the Si/C ratio of as-deposited films.

Sample label	Si (at%)	C (at%)	N (at%)	O (at%)	Si/C
Si-rich SiC	76.3	18.6	2.9	2,2	4.1
Stoichiometric SiC	44.0	44.1	5.6	6.3	1.0

Figures 2(a)–2(d) are the high resolution Si 2p and C 1s XPS spectra, which are shown with their deconvolution results, for the as-deposited stoichiometric and Si-rich SiC films. For the spectra of the Si-rich SiC film as shown in Figs. 2(a) and 2(b), two Gaussian peaks centered at 99.2 eV and 100.1 eV, decomposed from the Si 2p peak, could be attributed to Si–Si and Si–C bond, respectively.[18,19] The area percent of Si–Si bonds with binding energy 99.2 eV in this Si 2p peak is 78.6%, which indicates that the content of the extra silicon in this film is very high. On the other hand, the C 1s peak is best fitted only by a Gaussian peak centered at 282.7 eV, which can be assigned to the C–Si bond.[20,21]

For the spectra of the stoichiometric SiC film as shown in Figs. 2(c) and 2(d), three Gaussian peaks centered at 99.8 eV, 100.6 eV and 102.6 eV, decomposed from the Si 2p peak, could be attributed to Si–Si, Si–C and Si–O bonds, respectively.[22–24] The area percent of Si–Si bonds with binding energy 99.8 eV is 12.1%, which indicates the existence of silicon clusters. Three Gaussian peaks centered at 283.4 eV, 284.6 eV and 285.6 eV, decomposed from C 1s peak, could be attributed to C–Si, C–C and C–O bonds, respectively.[22–26]

And the area percent of C–C bonds with binding energy 284.6 eV is 14.8%, which indicates the existence of sp^2 C–C bonds of the graphite-like clusters.

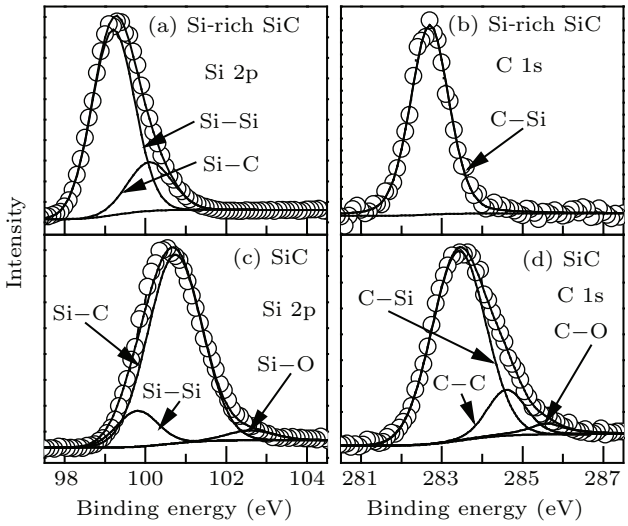


Fig. 2. The Si 2p and C 1s XPS spectra of the as-deposited stoichiometric and Si-rich SiC films, deconvolution of each spectrum with Gaussian peak is also shown in the figure.

3.2. Raman characterization

The Raman spectra of the as-deposited stoichiometric and Si-rich SiC films are shown in Fig. 3. The spectra of the as-deposited stoichiometric and Si-rich SiC film exhibit three and two main bands, respectively. Both bands centered on 475 cm^{-1} and 518 cm^{-1} are due to the Si–Si bonds and both bands centered on 810 cm^{-1} and 830 cm^{-1} are due to the Si–C bonds. The last band centered around 1440 cm^{-1} is due to the C–C bonds.[14,27] Comparing the Raman spectra shown in Figs. 3(a) and 3(b), besides Si–C bonds, the Si-rich SiC film contains Si–Si bonds, while the stoichiometric SiC film contains Si–Si and C–C bonds.

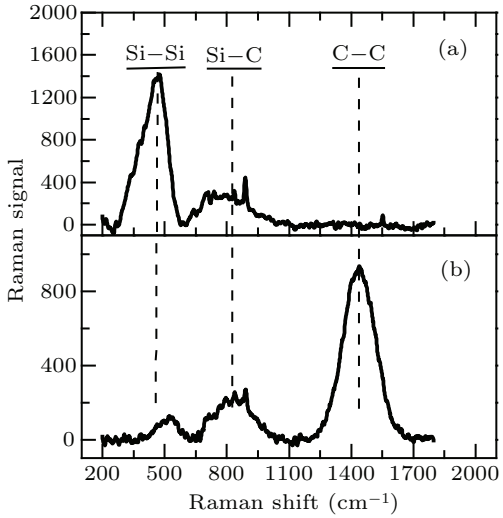


Fig. 3. The Raman spectra of the as-deposited Si-rich SiC (a) and stoichiometric SiC (b) films.

3.3. FT-IR characterization

Figure 4 shows the FT-IR spectra of the stoichiometric and Si-rich SiC films before and after oxidizing at different temperatures in air for 60 min. The spectra show two main overlapping peaks centered around 800 cm^{-1} and 1080 cm^{-1}, which are assigned to the stretching vibration mode of Si–C and Si–O bonds, respectively.[23,27] A little peak centered around 456 cm^{-1} is assigned to the rocking mode of Si–O bonds.[23,27]

It is known that a SiC film is oxidized when the absorption peak of Si–O bonds appears in its FT-IR absorption spectrum. Comparing Fig. 4(a) with 4(b), it is found that the stoichiometric SiC film begins to oxidize at 800 ° in air, while the Si-rich SiC film begins to oxidize at 900 °C in air. It is also known that the oxidation level of SiC film correlates positively with the integrated absorbance of the Si–O peak. In order to obtain the integrated absorbance of the Si–O peak, the absorption bands located at 400–1200 cm^{-1} are fitted by three Gaussian peaks: (1) the Si–C stretching vibration peak, (2) the Si–O stretching vibration peak, and (3) the Si–O rocking peak. And the typical fitting results of the stoichiometric and Si-rich SiC films oxidized at 1000 °C are given in Fig. 4.

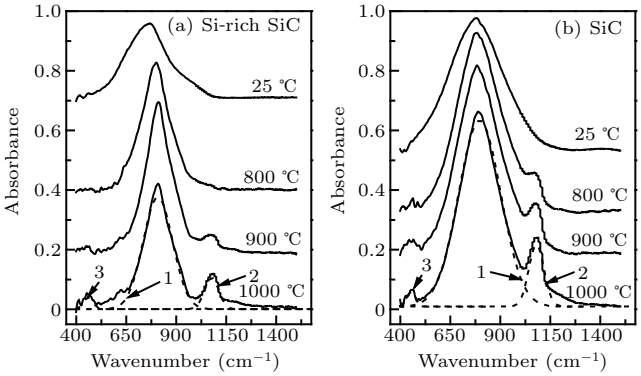


Fig. 4. The FT-IR spectra of the Si-rich SiC (a) and stoichiometric SiC (b) films, together with deconvolution results.

The integrated absorbance of Si–O peak is shown as a function of oxidation temperature in Fig. 5. For the Si-rich SiC oxidation films, the integrated absorbance of the Si–O peak increases from 5.6 to 9.3 with the oxidation temperature increasing from 900 °C to 1000 °C; for the stoichiometric SiC oxidation films, the integrated absorbance of the Si–O peak increases from 10.3 to 19.8 with the oxidation temperature increasing from 800 °C to 1000 °C. The integrated absorbance of the Si–O peak of the stoichiometric and Si-rich SiC films increases with increasing oxidation temperature, which means that the oxidation level of those films increases.

It can be obtained from Fig. 4 that the initial oxidation temperature of the Si-rich SiC film is 100 °C higher than that of the stoichiometric SiC film. Comparing the integrated absorbance of the Si–O peak of the stoichiometric films with that

of the Si-rich SiC films, we can find that the value of the integrated absorbance of the stoichiometric SiC film, which is 10.3 at oxidation temperature 800 °C, higher than 9.3 of the Si-rich SiC film at oxidation temperature 1000 °C and the value of the integrated absorbance of the stoichiometric SiC film (19.8 at oxidation temperature 1000 °C) is 2.1 times as high as 9.3 of the Si-rich SiC film at same oxidation temperature. Thus, the high-temperature anti-oxidation property of the Si-rich SiC film is better than that of the stoichiometric SiC film.

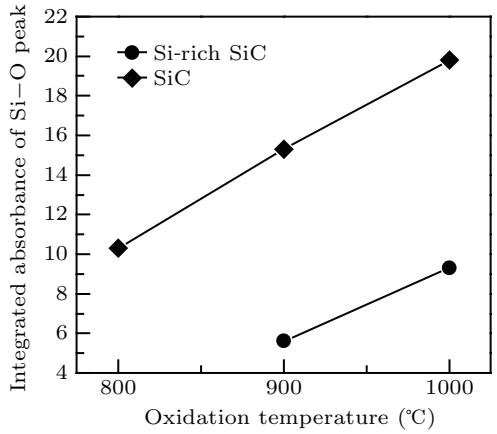


Fig. 5. The integrated absorbance of Si–O peak appeared in FT-IR spectra shown in Fig. 4 as a function of oxidation temperature.

Now we try to explain the anti-oxidation property difference between the stoichiometric and Si-rich SiC films. At the initial stage of oxidation, SiO_2 layer is formed on the film surface by oxidizing SiC film. As time goes by, more SiC is oxidized into SiO_2, and a continuous silica protective layer with low oxygen diffusion coefficient and good self-sealing property is gradually produced, thereby blocking the contact between oxygen and the SiC film and slowing down the oxidation rate of SiC film.

From above characterizations we can know that: (1) the Si-rich SiC film contains a large amount of extra silicon; (2) the stoichiometric SiC film contains graphite-like clusters. Due to the lower activation energy of Si than that of SiC, the oxidation rate of Si is 1.5–2 times higher than that of SiC.[28] For the Si-rich SiC films, when the oxidation temperature is higher than 800 °C, the large amount of extra silicon in the surface of the film can firstly be oxidized into SiO_2, and then a continuous silica protective layer is formed quickly, thus the oxidation rate of the Si-rich SiC film is limited by limiting the diffusion rate of oxygen. On the other hand, oxidation of the graphitic carbon by oxygen is thermodynamically favorable at temperatures above 500–600 °C. For the stoichiometric SiC films, when the oxidation temperature is higher than 800 °C, the graphite-like carbon clusters in the stoichiometric SiC films can easily be oxidized and removed from the films in the form of volatile carbon oxides. Such a process increases the porosity of the stoichiometric SiC films, and the diffusion rate of oxygen can be enhanced by increasing the porosity of the film, thus the oxidation rate of the stoichiometric SiC film is enhanced by enhancing the diffusion rate of oxygen.[11,12] In short, the high-temperature anti-oxidation property of the Si-rich SiC films is improved by the large amount of extra silicon, and the high-temperature anti-oxidation property of the stoichiometric SiC film is reduced by the graphite-like carbon clusters.

3.4. AFM characterization

Figures 6(a)–6(d) are the AFM surface morphology images of the stoichiometric and Si-rich SiC films before and after high temperature oxidation measured by tapping mode, and the scanned area is approximately 2×2 μm. From Fig. 6 we can see that both root mean square (RMS) roughness of the films decrease after high temperature oxidation: the RMS roughness of the stoichiometric SiC film decreases from 2.13 nm to 1.27 nm and that of the Si-rich SiC film decreases from 1.38 nm to 0.65 nm. The roughness decreases after high temperature oxidation for both films is reasonable considering the taper would be easier to be eroded in high temperature oxidation atmosphere. What is worth to note is that the roughness of the stoichiometric SiC film (1.27 nm) is about one time larger as compared with that of the Si-rich SiC film (0.65 nm) after high temperature oxidation, this larger difference might come from the fact that the C atoms in the stoichiometric SiC films were oxidized to carbon oxide and diffused out, leaving more voids than that of the Si-rich SiC films, in which the extra Si atoms were easily to be oxidized into a thin silica passivation layer as discussed in the next section.

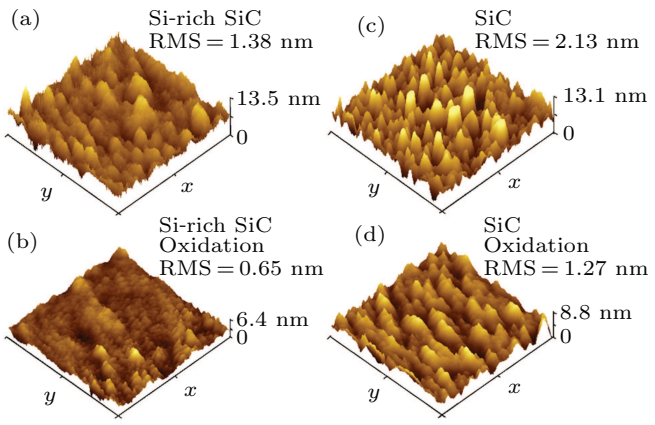


Fig. 6. The surface morphology images of the stoichiometric and Si-rich SiC films before (a), (c) and after (b), (d) high temperature oxidation.

3.5. Nano-indentation characterization

Figure 7 shows the hardness-indentation depth distribution curves of the stoichiometric and Si-rich SiC films before and after oxidizing at different temperature. It is shown in Figs. 7(a) and 7(e) that the hardness of the as-deposited stoichiometric and Si-rich SiC film increase with increasing in-

dentation depth in the range from 0 to 82 nm and keep almost constant in the flat range from 82 nm to 250 nm.

It is worth to note the different trends of hardness-indentation depth distribution curves of the stoichiometric and Si-rich SiC oxidation films. For the stoichiometric SiC oxidation films, a new step plateau appears in the range from 9 nm to 16 nm on the hardness-indentation depth curve of the 800 °C oxidation film, and this step plateau becomes obvious in the range from 13 nm to 23 nm on the curve of the 900 °C oxidation film and becomes wider in the range from 17 nm to 42 nm on the curve of the 1000 °C oxidation film. The hardness value of the step plateaus found in the stoichiometric SiC oxidation films is about 10 GPa, which is close to the hardness of silica.[29,30] Thus, we could conclude that the stoichiometric SiC films have been completely oxidized to silica in this step plateau regions, and the plateau is broadened with increasing oxidation temperature, meaning that the stoichiometric SiC films could be oxidized gradually in the depth direction at higher temperature in air. The thickness of silica layer on the surface of the stoichiometric SiC films oxidized at 900 °C and 1000 °C, estimated from the hardness-indentation depth distribution curves, are 23 nm and 42 nm, respectively.[31]

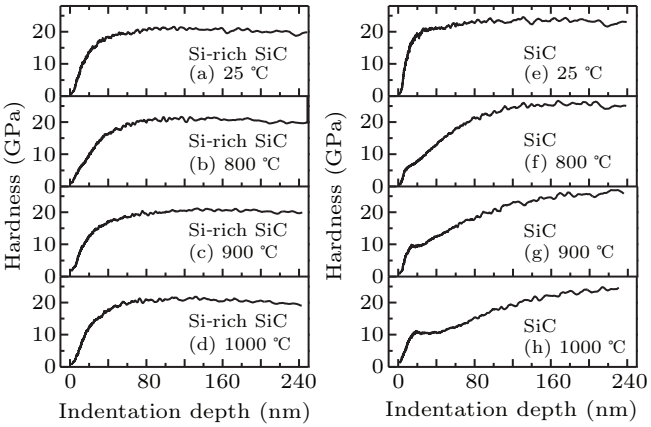


Fig. 7. The hardness-indentation depth distribution curves of the stoichiometric and Si-rich SiC films before and after oxidizing at different temperature.

Due to the relatively thick silica layer on the top of the stoichiometric SiC oxidation films, new changes could be observed on its hardness-indentation depth distribution curves; on the contrary, no such step plateau could be observed on the hardness-indentation depth distribution curves of the Si-rich SiC oxidation films. This phenomenon means that the silica layer on the top of the Si-rich SiC oxidation films is too thin to make any difference in nano-indentation characterization. Thus, the oxidation layer thickness of the Si-rich SiC film is thinner than that of the stoichiometric SiC film in the depth direction. The reason of increase of Si-rich SiC film's anti-oxidation performance might be the extra Si and lack of C in such film, extra Si is easier to be oxidized into silica and the lack of C reduces the voids, which would act as oxygen tunnel if there were too many voids forming in high temperature oxidation atmosphere after the C is oxidized into carbon oxide and diffuse out of the films, as discussed in stoichiometric SiC film.

4. Conclusion

The stoichiometric and Si-rich SiC films had been deposited on Si substrates by MW-ECR plasma enhanced RF magnetron sputtering method. The Si/C ratio of the stoichiometric and Si-rich SiC films is 1 and 4.1, respectively. The as-deposited Si-rich SiC film contains a large amount of extra silicon, while the as-deposited stoichiometric SiC film contains a small quantity of silicon and graphite-like clusters. Due to the thin protective silica layer with low oxygen diffusion constant formed by oxidizing the large amount of extra silicon, the high-temperature anti-oxidation property of the Si-rich SiC film is better than that of the stoichiometric SiC film. The anti-oxidation temperature of the Si-rich SiC film is 900 °C, which is 100 °C higher than that of the stoichiometric SiC film. After high temperature oxidation, both RMS roughness of the films decreases, and the RMS roughness of the stoichiometric SiC film (1.27 nm) is about two times higher than that of the Si-rich SiC film (0.65 nm). And the oxidation layer thickness of the Si-rich SiC film is thinner than that of the stoichiometric SiC film in the depth direction. Thus, the large amount of extra silicon can improve the anti-oxidation property of the Si-rich SiC film, which is beneficial to further improve the high-temperature anti-oxidation property of SiC film.

References

[1] Xu M, Girish Y R, Rakesh K P, Wu P, Manukumar H M, Byrappa S M, Udayabhanu and Byrappa K 2021 *Mater. Today Commun.* **28** 102533
[2] Liu P, Hao J L, Wang S K, You N N, Hu Q Y, Zhang Q, Bai Y and Liu X Y 2021 *Chin. Phys. B* **30** 077303
[3] He R, Zhou N, Zhang K, Zhang X, Zhang L, Wang W and Fang D 2021 *J. Adv. Ceram.* **10** 637
[4] Ning K and Lu K 2018 *J. Am. Ceram. Soc.* **101** 3662
[5] Huang L, Zhu J, Ma Y, Liang T, Lei C, Li Y and Gu X 2021 *Acta Phys. Sin.* **70** 207302 (in Chinese)
[6] Liu H, Li J and Li B 2018 *Chin. Phys. Lett.* **35** 096103
[7] Xu Y, Diao H, Zhang S, Li X, Zeng X, Wang W and Liao X 2007 *Acta Phys. Sin.* **56** 2915 (in Chinese)
[8] Bu A, Zhang Y, Zhang Y, Chen W, Cheng H, Wang L and Wang Y 2018 *Coatings* **8** 344
[9] Qiang X, Li H, Zhang N, Liu Y and Tian S 2018 *Int. J. Appl. Ceram. Technol.* **15** 1100
[10] Arce R, Koropecki R R, Buitrago R H, Alvarez F and Chambouleyron I 1989 *J. Appl. Phys.* **66** 4544
[11] Choi W K, Lee L P, Foo S L, Gangadharan S, Chong N B anf Tan L S 2001 *J. Appl. Phys.* **89** 1942
[12] Vasin A V, Muto S, Ishikawa Y, Rusavsky A V, Kimura T, Lysenko V S and Nazarov A N 2011 *Thin Solid Films* **519** 2218
[13] Jiang Y, Ru H, Ye C, Wang W, Zhang C and Su X 2018 *Ceram. Int.* **44** 17369
[14] Wang H, Zhang L, Lu W and Xu J 2020 *Plasma Sci. Technol.* **22** 034010

[15] Zhang Z, Liu T, Xu J, Deng X and Dong C 2006 *Surf. Coat. Technol.* **200** 4918

[16] Xu J, Deng X, Zhang J, Lu W and Ma T 2001 *Thin Solid Films* **390** 107

[17] Choi W K, Ong T Y, Tan L S, Loh F C and Tan K L 1998 *J. Appl. Phys.* **83** 4968

[18] Lin H, Gerbec J A, Sushchikh M and Mcfarland E W 2008 *Nanotechnology* **19** 325601

[19] Cheng C H, Wu C L, Lin Y H, Yan W L, Shih M H, Chang J H, Wu C I, Lee C K and Lin G R 2015 *J. Mater. Chem. C* **3** 10164

[20] Masuda T, Iwasaka A, Takagishi H and Shimoda T 2016 *J. Am. Ceram. Soc.* **99** 1651

[21] Kamble M, Waman V, Mayabadi A, Funde A, Sathe V, Shripathi T, Pathan H and Jadkar S 2017 *Silicon* **9** 421

[22] Khatami Z, Wilson P R J, Wojcik J and Mascher P 2017 *Thin Solid Films* **622** 1

[23] Ramos-Serrano J R, Matsumoto Y, Méndez-Blas A, Dutt A, Morales C and Oliva A I 2019 *J. Alloys Compd.* **780** 341

[24] Awad Y, Khakani M A EI, Aktik C, Mouine J, Camiré N, Lessard M, Scarlete M, Al-Abadleh H A and Smirani R 2009 *Surf. Coat. Technol.* **204** 539

[25] Wang L 2011 *J. Non-Cryst. Solids* **357** 1063

[26] Jedrzejowski P, Cizek J, Amassian A, Klemberg-Sapieha J E, Vlcek J and Martinu L 2004 *Thin Solid Films* **447** 201

[27] Khalfi A EI, Ech-chamikh E, Ijdiyaou Y, Azizan M, Essafti A, Nkhaili L, El Kissani A and Tomasella E 2017 *Vib. Spectrosc.* **89** 44

[28] Opila E J 1994 *J. Am. Ceram. Soc.* **77** 730

[29] Pöhlmann K, Bhushan B and Gahr K H Z 2000 *Wear* **237** 116

[30] Khakani M E, Chaker M, O'Hern M E and Oliver W C 1997 *J. Appl. Phys.* **82** 4310

[31] Saha R, Xue Z, Huang Y and Nix W D 2001 *J. Mech. Phys. Solids* **49** 1997